sciendo

CAIM
ISSN 2038-0909

Commun. Appl. Ind. Math. 15 (2), 2024, 17–27 DOI: 10.2478/caim-2024-0009

Review Article

Insights on neural signal analysis with Higuchi fractal dimension

Karolina Armonaite[1,2,3], Livio Conti[2], Elzbieta Olejarczyk[4], and Franca Tecchio[3]

[1]Faculty of Engineering, Uninettuno University, Rome, Italy
[2]INFN - Istituto Nazionale di Fisica Nucleare, Sezione Roma Tor Vergata, Rome, Italy
[3]Laboratory of Electrophysiology for Translational NeuroScience, Institute of Cognitive Sciences and Technologies - National Research Council, Rome, Italy
[4]Nalecz Institute of Biocybernetics and Biomedical Engineering Polish Academy of Sciences, Warsaw, Poland

[*]Email address for correspondence: karolina.armonaite@uninettunouniversity.net

Communicated by Alessandra De Rossi
Received on 06 28, 2024. Accepted on 08 26, 2024.

Abstract

Neurophysiological signal analysis is crucial for understanding the complex dynamics of brain function and its deviations in various pathological conditions. Traditional linear methods, while insightful, often fail to capture the full spectrum of inherently non-linear brain dynamics. This review explores the efficacy and applicability of the Higuchi fractal dimension (HFD) in interpreting neurophysiological signals such as scalp electroencephalography (EEG) and stereotactic intracranial encephalography (sEEG). We focus on three case studies: i) distinguishing between Alzheimer's disease (AD) and healthy controls; ii) classifying neurodynamics across diverse brain parcels looking for a signature of that cortical parcel; and iii) differentiating states of consciousness. Our study highlights the potential of non-linear analysis for deeper insights into brain dynamics and its potential for improving clinical diagnostics.

Keywords: `Higuchi fractal dimension, neural electrical activity, cerebral cortex`

1. Introduction

Investigations of the structure of human brain neural networks and their biophysical mechanisms suggest the hypothesis that the analysis of the ongoing neuronal electrical activity, the neurodynamics, measured via intracranial or scalp electroencephalography (sEEG/EEG), requires a non-linear measure approach [1]. It has been shown that brain signals often yield skewed, heavy-tailed distributions [2]. Such distributions indicate a scale-free dynamics or the existence of self-similar regularities that are expressed in a non-exact/statistical fractal geometry [3]. In the case of brain dynamics, such statistical self-similarity could be observed even at different time scales [4,5]. For this reason, the complexity of the patterns displayed in the electrical brain recordings requires means to detect the differences between the neurodynamics generating processes. In particular, it is clinically relevant to extend the analysis of neurodynamics from linear measures to non-linear ones, in order to evaluate the overall signal complexity across different conditions, as studies suggest that measures such as Hurst Exponent, Entropy, and Correlation Dimension are useful in detecting the reduced complexity of the neurodynamics in sleep/wake states [6,7] and sedation levels [8], as well as in pathological cases [9,10]. Furthermore, the fractal dimension index of neurophysiological signals has been proven to be sensitive to alterations in clinical scenarios such as stroke [11], Alzheimer's disease [12], and fatigue in multiple sclerosis [13]. Conversely, it has been shown to detect increased complexity in conditions like depression [14]. Moreover, it is useful to identify the fingerprint neurodynamics for different brain regions with complexity measures [15,16]. The scope of this review is to provide an overview of Higuchi fractal dimension (HFD) and its application for neurophysiological signal analysis in clinical settings.

2. Fractal features of neurodynamics

Mathematical fractal shapes are mostly generated by recursive algorithms that involve iterations; a transformation $T : X \to X$ is a function with domain X and codomain X. Then, $T^n(x)$ is a composite function $T^n(x) = \underbrace{T \circ T \circ \cdots \circ T(x)}_{\text{(n times)}} = T(T(\cdots T(x) \cdots))$. And the orbit of x is the sequence $O(x) = \{x, T(x), T^2(x), T^3(x), \ldots\}$. As a definition, for an object to be a fractal, it has to satisfy several conditions:

1. to possess a self-similarity of the shape, thus, generated through iterative process;
2. have a scale-free property;
3. to be a function that is continuous, but not differentiable;
4. to hold an irregularity of the shape [17,18].

Self-similarity can be defined in exact mathematical terms or through statistical self-similarity. An object exhibits exact mathematical self-similarity when each smaller part of the object is an ideal or nearly ideal replica of the entire object. Classic examples of geometrically self-similar objects include the curve introduced by Niels Fabian Helge von Koch, a complex geometrical structure that can hardly be described by Euclidean geometry, as it has a finite area and an infinite length [3]. The curve can be generated through an iterative process [5]. For example, generating Koch curves requires four affine transformations [19] and it has a non-integer dimension.

In Figure 1, we provide an example of Koch curve with its fractal dimension. The generation process is to begin with a straight-line segment (left panel); split the initial line segment into three equal parts, on the middle third of the line segment, construct an equilateral triangle pointing outwards (middle panel); draw two lines from the endpoints of the middle third segment, each at a 60-degree angle to the original segment; connect these two lines to form an equilateral triangle (right panel). The ideal scale-free behavior can be proved by the power-law property, from this geometrical distribution we can extract the fractal dimension of this shape using a self-similarity dimension. The D is calculated using the formula $D = \frac{\log(N)}{\log(S)}$, where N is the number of self-similar pieces and S is the scaling factor. The formula is derived from the fact that an object can be divided into N smaller parts, each of which is a scaled-down version of the entire object by a factor of S. Therefore, they follow the relationship: $N = S^D$. The Koch curve holds $D = \frac{\log(4)}{\log(3)}$.

Figure 1. The generating process of the Koch curve

When speaking about natural phenomenon, we often encounter fractal shapes that do not adhere exact mathematical fractal generation rules, but express some statistical properties of fractals. Examples include seismic activity described by the Gutenberg-Richter scale [20,21], solar electromagnetic storms [22,23], the connectivity of the cortical neural networks [5], and the irregular shape of the ongoing neural electrical activity, the neurodynamics [15,24–26]. To calculate the fractality of such time series is not straightforward as the self-similarity is statistical and it could be expressed at different time scales [4,27,28]. A primary indicator of scale-free activity, and thus possibly fractality, in neurophysiological time series is the power-law behaviour, expressed as the linear tendency of power spectral density (PSD) on a logarithmic scale [29,30]. As presented in Figure 2, the PSD of neural recordings from the cerebral cortex appears to follow a power-law distribution. On the log-log scale, it exhibits nearly linear behaviour indicating the existence of self-similarities in the neural electrical activity patterns.

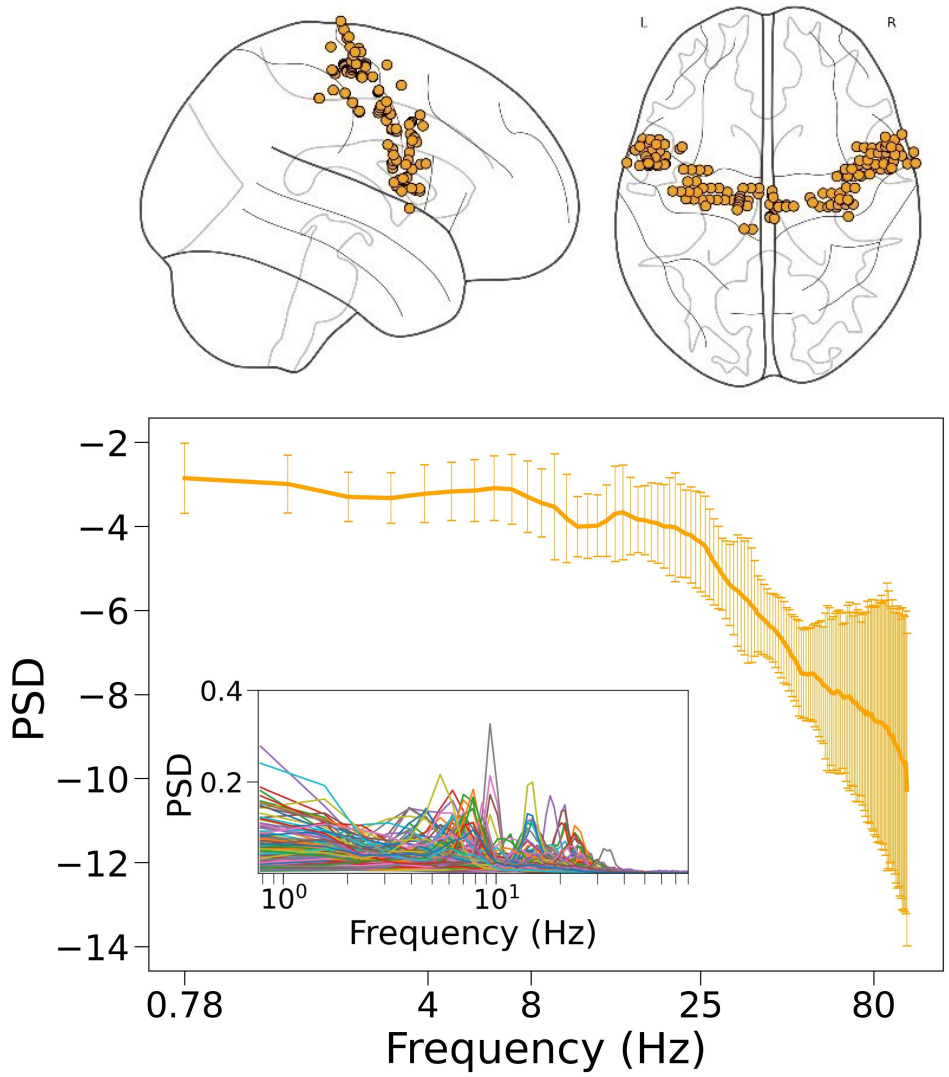

Figure 2. Top panel. The locations of the electrodes on the human cerebral cortex projected from sagittal and axial planes. Bottom panel. In the inset figure are shown the 141 PSDs of the neural recordings from the cerebral cortex. The x-axis is presented in logarithmic scale. In the main figure the mean of PSD of all channels is presented on log-log scale.

The PSD is calculated according to the Welch method. Start with segmentation of the time series $x_k[n] - x[n + k(L - D)]w[n]$, $k = 0, 1, \ldots, K - 1$, where $w[n]$ is the window function (e.g., Hamming). On each segment calculate a periodogram using a Fast Fourier Transform:

$$P_k(f) = \frac{1}{U} \left| \sum_{n=0}^{L-1} x_k[n] e^{-j2\pi f n} \right|^2 .$$

Then average across the periodograms:

$$P_{\text{Welch}}(f) = \frac{1}{K}\sum_{k=0}^{K-1} P_k(f).$$

However, the linear measures like Fourier Transform might fall short in detecting the existing non-linearities in neurophysiological signals [31]. For this reason, here, we provide a plausible method to capture the complex features in the neural signals, directly from time domain, for this we deploy the Higuchi fractal dimension.

3. Higuchi fractal dimension

The time series like Earth electromagnetic field activity was shown to express high irregularities, and the method to estimate the size of such fluctuations was shown by T. Higuchi (1988) [32]. He suggested to subsample the time series into a shorter series of some length. Consider a given N-length time series $\{X(1), X(2), X(3), \ldots, X(N)\}$. For a time interval, we skip a number of samples equal to k. We obtain m number of sets of new time series X_k^m: $X(m), X(m+k), X(m+2k), \ldots, X(m+[(N-m)/k])$. Then we calculate the length of the curve X_k^m as follows:

$$L_m(k) = \frac{\left[\sum_{i=1}^{\lfloor (N-m)/k \rfloor} |X(m+ik) - X(m+(i-1)k)|\right](N-1)}{\lfloor (N-m)/k \rfloor \cdot k} \cdot \frac{1}{k}$$

The length $L(k)$ of the newly generated subseries X_k^m is evaluated by averaging the k sets of $L_m(k)$ values, as:

$$L(k) = \frac{1}{k}\sum_{m=1}^{k} L_m(k)$$

If the limit exists for $k \to \lfloor N/2 \rfloor$, such as:

$$L(k) \propto k^{-HFD}$$

then the curve is fractal with dimension equal to $HFD(f, N, k_{\max}) = a$.

4. Review of three HFD applications for measuring neurodynamics complexity

Here, we provide an overview of some cases of Higuchi's algorithm application in detecting the complexity of neurophysiological signals, across healthy and pathological conditions, across different cortical parcels and consciousness states.

4.1. *Case 1: reduced HFD in Alzheimer's disease and aging*

In the study by Smits et al. 2016, Authors calculated HFD on 5-minutes duration, 19 - channel scalp EEG recordings, sampled at 128 Hz, from 41 healthy individuals (20-89 y.o.) and 67 Alzheimer's Disease (AD) patients (50-88 y.o.). The elderly healthy control (EC) group and AD patients were tested by Mini Mental State Examination score (MMSE) and a Non-Ceruloplasmin-Bound Copper Levels (NCC) for cognitive decline symptoms. The aim was to determine if HFD can detect changes in brain activity of healthy aging and AD with respect to young controls. The results showed a non-linear relationship between HFD and age in healthy individuals ($R^2 = .575, p < 0.001$). HFD expressed a declination around age of 60, with the reduction noticeable in the central-parietal regions more pronounced in the right hemisphere compared to the left ($p = 0.006$). Moreover, a correlation between HFD and MMSE score was also found (the significance threshold, ($r = 0.264, p = 0.031$), furthermore a linear relationship between HFD and NCC levels was shown ($r = -0.274, p = 0.025$). In the Figure 3 we present these results. In the panel A the dots represent the average whole-scalp HFD values from left to right: healthy subjects

plotted against age in years with the best fitting curve; AD patients plotted against MMSE scores; AD patients plotted against NCC levels, with the best fitting line. For the comparisons of HFD of the three groups, it was noticed that AD patients exhibited lower HFD compared to aged and young controls. In the Figure 3 B the reduction of average HFD values for the left and right parietal regions for each group can be noticed. This reduction was linked to decreased cognitive capabilities decline, as measured by the mini-mental state examination, and NCC levels. These findings indicate that the complexity of resting-state EEG increases from young age to adulthood and decreases in healthy aging. In AD, the complexity of brain activity is further reduced in association with loss of cognition. Summarizing, HFD appears to be a reliable measure for monitoring EEG-derived brain activity complexity in both healthy and pathological aging.

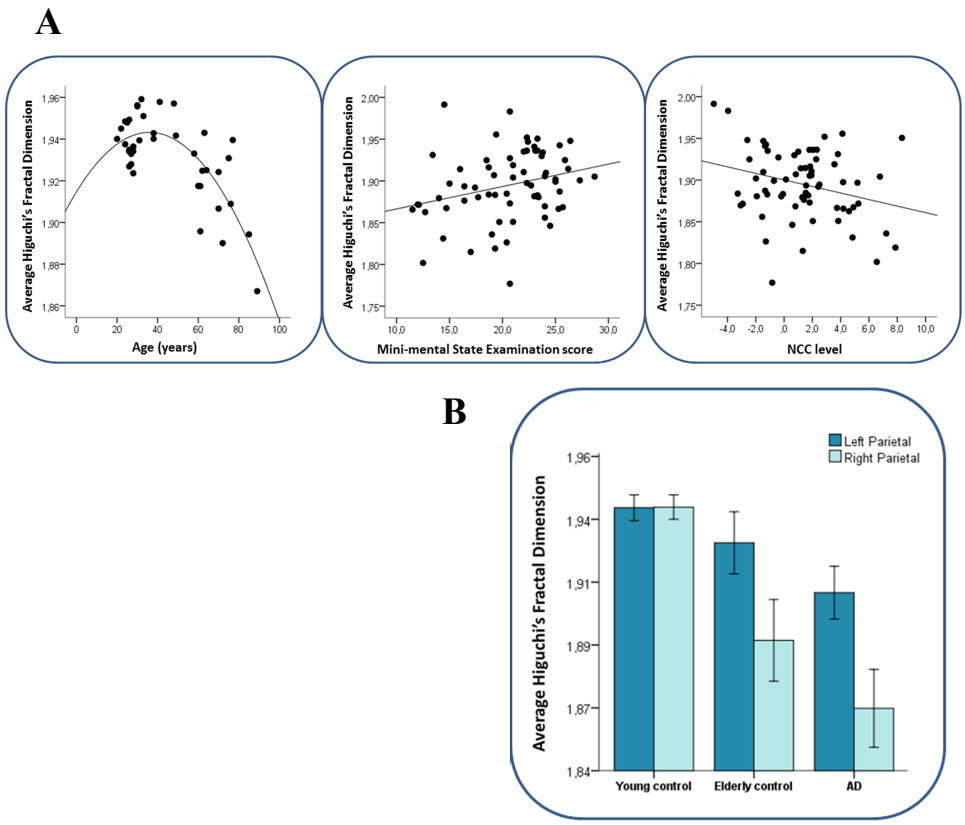

Figure 3. A. Correlation of HFD and various parameters. B. HFD across three groups of investigation.[Figure reprinted from Smits et al., 2016, PLOS ONE, DOI:10.1371/journal.pone.0149587]

4.2. *Case 2: HFD as a fingerprint of brain areas neurodynamics in resting wakefulness*

In the following two studies, HFD was applied to analyse if local brain areas neurodynamics exhibit characteristic activity in resting wakefulness [15,16]. In both studies, Authors used sEEG recordings from Montreal Neurological Institute (MNI) of 106 subjects suffering from drug-resistant focal epilepsy, however the regions affected by the disease were excluded from the study. In the analysis by Olejarczyk et al., 2022 [16], Authors estimated the average HFD across all channels and all subjects in 38 brain regions. They observed some significant differences across brain regions, where the highest HFD was noticed in the frontal cortex, in particular, the two areas were found to be active during wakefulness: the middle segment of the precentral gyrus and the inferior segment of the inferior frontal gyrus. Both expressed HFD greater than 1.7 ± 0.1 (Figure 4 top panel). Where the highest HFD is observed in the frontal lobe, the lowest in parahippocampal and fusiform gyri. In the second study by Armonaite et al. [15,33], authors selected three regions: primary motor (M1), primary somatosensory (S1), and primary auditory (A1) cortices for the investigation, and examined if the differences in neurodynamics complexity across brain regions remain constant within a single subject. Deploying a non-parametric Wilcoxon test (Wtest), it was verified that $M1 \geq S1$ ($Wtest = 12, p = 0.01$), $M1 \geq A1$ in 8/9 subjects, and $S1 \geq A1$ in 5/6 subjects within a single subject. As presented in the Figure 4 bottom panel, the scatterplots of each subject's HFD values indicate where the two sources differ: S1 vs. M1; A1 vs. M1; A1 vs. S1. The diagonal and coloured areas indicate where the HFD of the source on the x-axis is higher than that on the y-axis.

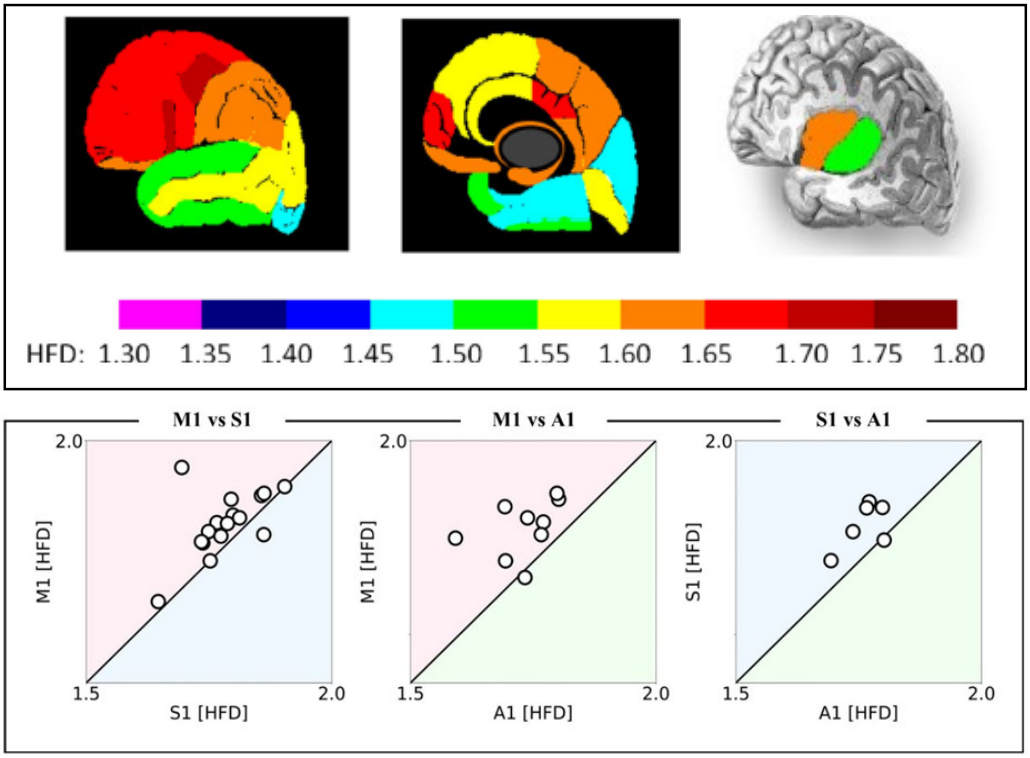

Figure 4. HFD of different brain areas in wakefulness. The results are shown on lateral, medial, and insular views from left to right. [Modified figure is reprinted from Olejarczyk et al., Nat. Sci. Rep, 2022, DOI : $10.1038/s41598-021-04213-8$]. B. HFD comparisons in three cortical parcels within a subject. Colour codes: $S1(blue), M1(red), A1(green)$. [Figure is reprinted from Armonaite et al., Advances in Neurobiology, 2024, DOI : $10.1007/978-3-031-47606-8_33$]

4.3. *Case 3: HFD is able to detect the consciousness states*

There are plenty of evidence suggesting that with consciousness states decrease either during Non-rapid-eye-movement (NREM) sleep or during anaesthesia [7,30] the brain regions become more synchro-

nized on a larger scale [34,35] and therefore exhibit slower periodic oscillations such as $\delta\,[\leq 4$ Hz] and $\theta\,[4-8$ Hz], than in wakefulness, where $\alpha\,[8-12$ Hz] and $\beta\,[12-33$ Hz] frequencies dominate [36,37]. Here, as for the brain areas classification, authors proceeded to look if Higuchi's method is able to capture these changes across the sleep staging and wakefulness. In both studies, it was noticed that HFD decreases from REM stage to N2 and N3. In particular in the study of Olejarczyk et al., 2022 [16] they found that in almost all of the 38 brain regions the complexity measured via HFD is reduced from wake to N3 sleep stage, however in many brain regions, wake state and REM sleep are more similar. Interestingly, the precentral gyrus showed differences in HDF between the wake state and REM sleep stage. Instead, the fusiform and parahippocampal gyri did not exhibit differences between the awake state and N2. Moreover, similarity in HFD was observed between stages REM and N2 only for the postcentral gyrus, the area containing the primary somatosensory cortex. The differences of the cortical areas with respect to sleep stages can be seen in the Figure 5 top panel. On the other hand, in the study by Armonaite et al., 2022 [38], authors selected three regions and showed how the complexity from the wake state to the N3 sleep stage decreases measured via HFD linearly correlating it with the PSD in δ frequency band since it has the most evident indication of sleep stages [7]. The steepness of the slope (α) was estimated, with the scope to examine if there is a negative correlation between HFD and δ frequency band, this would indicate that with the depth of sleep the HFD decreases significantly. In fact, it was found that the α value, was not only decreasing as with the depth of sleep, but also was different across A1, S1 and M1 measuring on single subjects and on average. The most evident decrease of HFD value as PSD(δ) increases is in A1. The Pearson's correlation (r) was evaluated for the significance of the fit of HFD versus PSD(δ) for a representative channel for each subject in wakefulness and sleep stages in three regions separately. The correlations were significant as follows: for A1 ($r = -0.824, p = 0.003$), for S1 ($r = -0.491, p = 0.045$), for M1 ($r = -0.669, p = 0.001$).

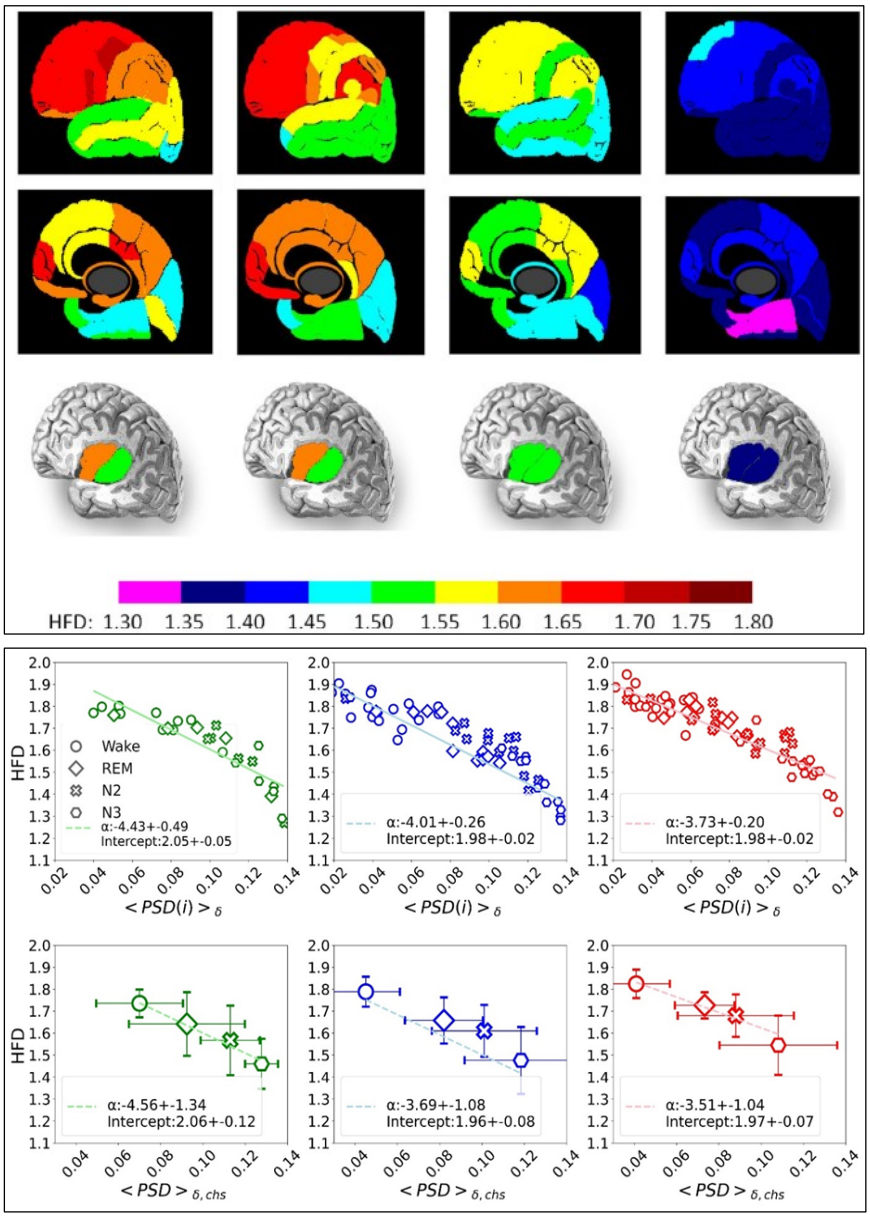

Figure 5. Top panel. HFD across sleep stages in different brain regions. The results are displayed on lateral, medial, and insular views from top to bottom rows, and from wake to N3 sleep stage shown from left to right. [Modified figure is reprinted from Olejarczyk et al., Nat. Sci. Rep, 2022, DOI: 10.1038/s41598-021-04213-8]. Bottom panel. HFD versus PSD δ mean band values in single subjects across the states. The top row represents each subject's HFD value versus PSD δ band mean value during wakefulness, REM, N2, and N3 sleep stages. In the bottom row, the mean of the HFD versus mean PSD(δ) across the population is shown.

5. Conclusion

While frequency domain analysis provides invaluable insights into periodicities across brain regions, it is limited to detecting the rate of neuronal activations in response to stimuli at the cellular level or the connections between large-scale brain regions at the network level. However, fluctuations in neural networks arise from various factors such as inhibitory/excitatory projections, internal neuronal "noise" produced by biophysical processes, and potentially the number of connections with other neurons in the neuronal pool. The Higuchi method could be a more sensitive tool for detecting such nonlinearities on a larger scale, making it a plausible estimator for identifying neurodynamical differences between brain regions, assessing sleep stages, and potentially serving as a marker for the deterioration of specific brain area functions. Although HFD has shown success in detecting these properties in neurophysiological signals, it requires further evaluation to understand its effectiveness across different time scales and with varying parameters.

References

1. N. J. Kopell, H. J. Gritton, M. A. Whittington, and M. A. Kramer, Beyond the connectome: The dynome, *Neuron*, vol. 83, pp. 1319–1328, sep 2014.
2. G. Buzsaki and K. Mizuseki, The log-dynamic brain: how skewed distributions affect network operations, *Nat Rev Neurosci*, vol. 15, no. 4, pp. 264–278, 2014.
3. A. Eke, P. Herman, L. Kocsis, and L. R. Kozak, Fractal characterization of complexity in temporal physiological signals, *Physiological Measurement*, vol. 23, no. 1, 2002.
4. B. J. He, J. M. Zempel, A. Z. Snyder, and M. E. Raichle, The temporal structures and functional significance of scale-free brain activity, *Neuron*, vol. 66, no. 3, pp. 353–369, 2010.
5. A. Di Ieva, *The Fractal Geometry of the Brain: An Overview.* Springer Series in Computational Neuroscience, 2016.
6. Y. Ma, W. Shi, C. K. Peng, and A. C. Yang, Nonlinear dynamical analysis of sleep electroencephalography using fractal and entropy approaches, *Sleep Medicine Reviews*, vol. 37, pp. 85–93, 2018.
7. M. Schartner, A. Seth, Q. Noirhomme, M. Boly, M. A. Bruno, S. Laureys, and A. Barrett, Complexity of multi-dimensional spontaneous EEG decreases during propofol induced general anaesthesia, *PLoS ONE*, vol. 10, no. 8, pp. 1–21, 2015.
8. R. Ferenets, T. Lipping, A. Anier, V. Jäntti, S. Melto, and S. Hovilehto, Comparison of entropy and complexity measures for the assessment of depth of sedation, *IEEE Transactions on Biomedical Engineering*, vol. 53, no. 6, pp. 1067–1077, 2006.
9. N. Kannathal, U. R. Acharya, C. M. Lim, and P. K. Sadasivan, Characterization of EEG - A comparative study, *Computer Methods and Programs in Biomedicine*, vol. 80, no. 1, pp. 17–23, 2005.
10. M. J. Cook, A. Varsavsky, D. Himes, K. Leyde, S. Berkovic, T. O'Brien, and I. Mareels, The dynamics of the epileptic brain reveal long memory processes, *Frontiers in Neurology*, vol. 5, no. OCT, pp. 1–8, 2014.
11. F. Zappasodi, E. Olejarczyk, L. Marzetti, G. Assenza, V. Pizzella, and F. Tecchio, Fractal dimension of EEG activity senses neuronal impairment in acute stroke, *PLoS ONE*, vol. 9, p. e100199, jun 2014.
12. F. M. Smits, C. Porcaro, C. Cottone, A. Cancelli, P. M. Rossini, and F. Tecchio, Electroencephalographic fractal dimension in healthy ageing and Alzheimer's disease, *PLoS ONE*, vol. 11, p. e0149587, feb 2016.
13. C. Porcaro, C. Cottone, A. Cancelli, P. M. Rossini, G. Zito, and F. Tecchio, Cortical neurodynamics changes mediate the efficacy of a personalized neuromodulation against multiple sclerosis fatigue, *Scientific Reports*, vol. 9, dec 2019.
14. M. Ahmadlou, H. Adeli, and A. Adeli, Fractality analysis of frontal brain in major depressive disorder, *International Journal of Psychophysiology*, vol. 85, no. 2, pp. 206–211, 2012.
15. K. Armonaite, M. Bertoli, L. Paulon, E. Gianni, M. Balsi, L. Conti, and F. Tecchio, Neuronal Electrical Ongoing Activity as Cortical Areas Signature: An Insight from MNI Intracerebral Recording Atlas, *Cerebral Cortex*, nov 2021.
16. E. Olejarczyk, J. Gotman, and B. Frauscher, Region-specific complexity of the intracranial EEG in the sleeping human brain, *Scientific reports*, vol. 12, dec 2022.
17. P. Bak, C. Tang, and K. Wiesenfeld, Self-organized criticallity, *Physical Review Letters*, vol. 38, no. 1, pp. 364–375, 1988.
18. K. Falconer, *Fractal and Applications Mathematical Foundations Geometry.* Wiley, 2003.
19. M. Rani, R. U. Haq, and D. K. Verma, Variants of Koch curve : A Review, *International Journal of Computer Applications® (IJCA)*, vol. 2, no. d, pp. 20–25, 2012.
20. K. Dahmen, D. ErtaÅŸ, and Y. Ben-Zion, Gutenberg-Richter and characteristic earthquake behavior in simple mean-field models of heterogeneous faults, *Physical Review E - Statistical Physics, Plasmas, Fluids, and Related Interdisciplinary Topics*, vol. 58, no. 2, pp. 1494–1501, 1998.
21. D. Legrand, The bodily self: The sensori-motor roots of pre-reflective self-consciousness, in *Phenomenology and the Cognitive Sciences*, pp. 89–118, Springer, mar 2006.

22. D. Hughes, M. Paczuski, R. O. Dendy, P. Helander, and K. G. McClements, Solar Flares as Cascades of Reconnecting Magnetic Loops, *Physical Review Letters*, vol. 90, no. 13, p. 4, 2003.
23. V. I. Abramenko, Self-Organized Criticality of Solar Magnetism, *Geomagnetism and Aeronomy*, vol. 60, no. 7, pp. 801–803, 2020.
24. W. Klonowski, E. Olejarczyk, and R. Stepien, Complexity of EEG-signal in Time Domain - Possible Biomedical Application, in *EXPERIMENTAL CHAOS: 6th Experimental Chaos Conference*, pp. 155–162, AIP Publishing, feb 2003.
25. C. Cottone, C. Porcaro, A. Cancelli, E. Olejarczyk, C. Salustri, and F. Tecchio, Neuronal electrical ongoing activity as a signature of cortical areas, *Brain structure function*, vol. 222, pp. 2115–2126, jul 2017.
26. F. Tecchio, M. Bertoli, E. Gianni, T. L'Abbate, L. Paulon, and F. Zappasodi, To Be Is To Become. Fractal Neurodynamics of the Body-Brain Control System, *Frontiers in Physiology*, vol. 11, dec 2020.
27. K. J. Miller, L. B. Sorensen, J. G. Ojemann, and M. den Nijs, ower-Law Scaling in the Brain Surface Electric Potential, *PLoS Computational Biology*, pp. Issue 12, Plos Computational Biology, 2009.
28. B. J. He, Scale-free brain activity: Past, present, and future, 2014.
29. P. Allegrini, D. Menicucci, R. Bedini, L. Fronzoni, A. Gemignani, P. Grigolini, B. J. West, and P. Paradisi, Spontaneous brain activity as a source of ideal 1/f noise, *Physical Review E - Statistical, Nonlinear, and Soft Matter Physics*, vol. 80, no. 6, pp. 1–13, 2009.
30. S. D. Muthukumaraswamy and D. T. Liley, 1/F Electrophysiological Spectra in Resting and Drug-Induced States Can Be Explained By the Dynamics of Multiple Oscillatory Relaxation Processes, *NeuroImage*, vol. 179, no. November 2017, pp. 582–595, 2018.
31. S. Kesić and S. Z. Spasić, Application of Higuchi's fractal dimension from basic to clinical neurophysiology: A review, *Computer Methods and Programs in Biomedicine*, vol. 133, no. May 2016, pp. 55–70, 2016.
32. T. Higuchi, Approach to an irregular time series on the basis of the fractal theory, *Physica D: Nonlinear Phenomena*, vol. 31, pp. 277–283, jun 1988.
33. K. Armonaite, L. Conti, and F. Tecchio, *Fractal Neurodynamics*, vol. 36. Springer Link, 2024.
34. M. Steriade, D. A. McCormick, and T. J. Sejnowski, Thalamocortical oscillations in the sleeping and aroused brain, *Science*, vol. 262, no. 5134, pp. 679–685, 1993.
35. C. G. Horváth, O. Szalárdy, P. P. Ujma, P. Simor, and F. Gombos, Overnight dynamics in scale â€‘ free and oscillatory spectral parameters of NREM sleep EEG, *Scientific Reports*, pp. 1–12, 2022.
36. B. Frauscher, N. von Ellenrieder, R. Zelmann, C. Rogers, D. K. Nguyen, P. Kahane, F. Dubeau, and J. Gotman, High-Frequency Oscillations in the Normal Human Brain, *Annals of Neurology*, vol. 84, pp. 374–385, sep 2018.
37. N. von Ellenrieder, J. Gotman, R. Zelmann, C. Rogers, D. K. Nguyen, P. Kahane, F. Dubeau, and B. Frauscher, How the Human Brain Sleeps: Direct Cortical Recordings of Normal Brain Activity, *Annals of Neurology*, vol. 87, pp. 289–301, feb 2020.
38. K. Armonaite, L. Nobili, L. Paulon, M. Balsi, L. Conti, F. Tecchio, K. Armonaite, L. Nobili, L. Paulon, M. Balsi, L. Conti, and F. Tecchio, Local neurodynamics as a signature of cortical areas: new insights from sleep, *Cerebral cortex (New York, N.Y. : 1991)*, jul 2022.